Available online at www.sciencedirect.com

Catalysis Today 107–108 (2005) 181–191

www.elsevier.com/locate/cattod

# SCR of NO with methane over Co-HBEA and PdCo-HBEA catalysts
## The promoting effect of steaming over bimetallic catalyst

A.P. Ferreira [a], C. Henriques [b,*], M.F. Ribeiro [b], F.R. Ribeiro [b]

[a] *Instituto Superior de Ciências da Saúde-Sul, 2825 Monte da Caparica, Portugal*
[b] *Departamento de Engenharia Química, Instituto Superior Técnico, Av. Rovisco Pais, 1049-001 Lisboa, Portugal*

**Abstract**

Ion-exchanged Co and PdCo-BEA zeolite-based catalysts were studied for the selective catalytic reduction (SCR) of NO with methane under oxygen excess. Bimetallic samples were submitted to several hydrothermal treatments (steaming) and tested under dry and wet conditions (2% $H_2O$). These hydrothermal treatments resulted in significant modifications in the amount and distribution of metal species, namely an increase of Co oxides and Co-oxo species, simultaneously with the preservation of $Co^{2+}$ isolated exchanged cations. $H_2$-TPR measurements detected, on these catalysts, a fraction of Co species more easily reducible, eventually interacting with Pd species and possibly related to dispersed nanosized oxide species, placed in more accessible positions. All the steamed catalysts exhibit a higher NO conversion into $N_2$ and an increased water resistance. The Co and/or Co-Pd species formed during steaming treatment, the balance between them and the framework dealumination are important issues for the high and stable catalyst activity under the presence of water vapor.

*Keywords:* $DeNo_x$; Co-BEA; PdCo-BEA; Steaming; Dealumination

## 1. Introduction

Growing concerns with environment in industrialized countries leads to more stringent values of the emissions of nitrogen oxides (NO, $NO_2$). The ideal catalyst for NO reduction should be active in a wide window of temperatures, resistant to a considerable amount of water in gas stream and to poisons (like sulfur) and should remain active for a long period of time.

Metal-exchanged zeolite catalysts are known to be active for the selective catalytic reduction (SCR) of $NO_x$ with hydrocarbons, in the presence of oxygen excess [1–3]. Recent works on catalysis by transition metal-exchanged zeolites indicate that the specific activity of active species (isolated metal ions, clusters, oxides) greatly depend on their location inside the network of cavities or even in the external surface of zeolite crystallites [4,5].

Co-zeolites have been studied in SCR reaction with methane, presenting a quite promising behavior [3,6]. However, when tested in the presence of water, these catalysts show a significant loss of activity in $NO_x$ conversion and a decrease of stability. Bimetallic Pd-Co zeolites have been tested and they revealed an increase of activity and stability when compared with monometallic Co catalysts [7–11]. However, they still show a significant loss of activity when water is present in the reaction mixture. Their catalytic activity is normally restored (at least partially) when water is suppressed, indicating a competitive adsorption in active sites. Nevertheless, some authors [4,12,13] have reported for Cu-MFI, Co-MFI and Co-Beta catalysts an enhancement of catalytic activity for NO reduction after hydrothermal treatments. This improvement in performances for NO reduction by $CH_4$ has been attributed to a redistribution of Co ions over the different zeolite exchange sites, usually assigned as α, β and γ. Co-BEA zeolites have been tested in the SCR of NO with methane which revealed poor results. On the contrary, studies performed in the presence of propane showed to be promising [14].

---

* Corresponding author. Tel.: +351 218417325; fax: +351 218419198.
*E-mail address:* pccarlos@alfa.ist.utl.pt (C. Henriques).

0920-5861/$ – see front matter © 2005 Elsevier B.V. All rights reserved.
doi:10.1016/j.cattod.2005.07.089

Table 1
Catalysts designation and hydrothermal treatments conditions

| Catalyst | Designation | Steaming temperature (°C) | Water vapor on steaming (vol.%) |
|---|---|---|---|
| Co (2%)-HBEA | Co-HBEA | – | – |
| Pd (0.15%) Co (2%)-HBEA | PdCo-HBEA | – | – |
| Pd (0.15%) Co (2%)-HBEA | st410 | 400 | 10 |
| Pd (0.15%) Co (2%)-HBEA | st510 | 500 | 10 |
| Pd (0.15%) Co (2%)-HBEA | st520 | 500 | 20 |

Co wt.% = 2; Pd wt.% = 0.15.

The reaction pathway of NO SCR with $CH_4$ is complex: although subjected to numerous studies, the reaction mechanism is still under debate. Several types of mechanisms have been suggested and $NO_2$ formation is claimed as the first key step in reaction mechanisms. These mechanisms seem to involve different catalytic functions [15–18], which suggests that an appropriate balance of the suitable catalytic sites should be a fundamental goal in order to obtain an active and stable catalyst.

The present work consists of the study of Co and PdCo-HBEA catalysts in the RCS of NO with methane in oxygen excess. The positive effect of the presence of water in the feed mixture, detected with the bimetallic catalyst, led us to submit it to more severe hydrothermal treatments, analogous to the steaming treatments usually used for zeolites dealumination. Moreover, dealumination of BEA zeolite has been reported to occur very easily [19] and several studies have demonstrated the beneficial effect of steaming on the performances of BEA zeolite [20–23]. The evaluation of the catalytic activity, selectivity and stability, in the presence of water vapor, as well as the effect of catalysts steaming are the main objectives of this work.

## 2. Experimental

### 2.1. Catalyst preparation

$NH_4$-BEA zeolite with Si/Al = 12.5 was provided by Zeolyst International. The Co-zeolite form was obtained by ion-exchanging the acidic form with a 0.032 M $Co(CH_3COO)_2$ solution at 80 °C for 24 h, under strong agitation. The catalyst was then thoroughly washed with distilled water and dried at 100 °C overnight. The procedure was followed by calcination at 500 °C (3 h) under air flow ($4\ L\ h^{-1}\ g^{-1}$) with a heat rate of 5 °C/min. This catalyst has 2 wt.% Co. Palladium was introduced by ion-exchange the calcinated Co-HBEA with the required amount of a solution of $Pd(NH_3)_4(NO_3)_2$ to obtain 0.15 wt.% Pd. This exchange occurs at room temperature during 24 h under a strong agitation. The catalyst was subsequently thoroughly washed with distilled water and dried at 100 °C overnight. This procedure was followed by calcination at 450 °C (8 h) under air flow ($4\ L\ h^{-1}\ g^{-1}$) with a heat rate of 1 °C/min.

Bimetallic catalyst was submitted to three different pre-treatments of calcination in the presence of water vapor (steaming). Steaming occurs under air, with a total flow rate of $30\ L\ h^{-1}\ g^{-1}$, during 3 h, at different conditions (see details in Table 1). After pre-treatments, catalysts were kept at 500 °C for 1 h under air flow.

### 2.2. Catalyst characterization

Catalysts chemical composition was determined by ICP analysis. Results are listed in Table 1.

Samples crystallinity, after exchange and steaming treatments, was evaluated by X-ray diffraction (XRD), in a Rigaku diffractometer with an incident radiation corresponding to the Cu Kα radiation.

$H_2$-temperature programmed reduction (TPR) experiments were performed using samples of 130 mg of catalyst (dry basis), heated from room temperature to 900 °C (bimetallic samples) or 1000 °C (monometallic sample) at 7.5 °C/min, under a mixture of $H_2$/Ar (5%) with a flow rate of $1.5\ L\ h^{-1}$. Hydrogen consumption was measured with a thermal conductivity detector (TCD); water was trapped in an ice-cooled trap.

Diffuse reflectance (DRS) UV–vis spectra were obtained in a UV spectrometer Shimadzu MPC 3100 equipped with a diffuse reflectance attachment that possesses an integrating sphere coated with $BaSO_4$. Spectra were recorded at a medium speed, with a slit width 5 nm and a sampling interval equal to 1. The absorption intensity was calculated from Kubelka–Munk theory where $F(R_\infty)$ is proportional to the absorption coefficient. All samples were dehydrated before the analysis and kept under vacuum atmosphere until the analysis was completed, in order to avoid Co ions to coordinate with water molecules [24].

Catalysts dealumination was evaluated by FTIR, with wafers obtained by dilution of the catalysts samples in dry KBr (1:100). Spectra were recorded in a Nicolet Nexus FTIR spectrometer (60 scans, resolution $4\ cm^{-1}$). Dealumination was determined following the procedure described elsewhere [25,26], using the correlation between the wavenumber of the frequency of asymmetric stretching vibration ($\sim 1090\ cm^{-1}$) and the number of framework Al atoms per unit cell.

### 2.3. Reaction system

The reduction of NO by methane in the presence of oxygen excess was carried out in a fixed-bed flow reactor, typically with 170 mg of catalyst. A gas mixture containing

1000 ppm NO, 2000 ppm $CH_4$, 5 vol.% $O_2$, 2 vol.% $H_2O$ and He balance was fed at a flow rate of 15 L $h^{-1}$, through Brooks mass flow-meters. The corresponding GHSV was 45,000 $h^{-1}$, considering catalysts bulk density of 0.5 g $cm^{-3}$. Catalysts were pre-treated under He at 500 °C (heat rate of 5 °C/min) for 1 h and were then cooled to the reaction temperature and kept in contact with the gas mixture for 1 h before the first analysis. Catalytic tests were then carried out for 2 h for each temperature, in a range between 350 °C and 550 °C. The compositions of feed and effluent gases were analyzed by using an on-line gas chromatograph (HP 5890 Series II) with two columns, MolSieve 5A for $N_2$, $O_2$, CO and $CH_4$ and Poraplot Q for $CO_2$ and two detectors assembled in series. TCD detector was used to detect $N_2$, $O_2$, CO and $CO_2$ and FID detector was used to monitor hydrocarbons. When the reaction was carried out in wet conditions (2% $H_2O$), the mixture was passed through an ice-cooled trap, prior to chromatograph, in order to remove most of the water contained in the gas stream.

Catalytic tests occurred in the following sequence: (1) a run under dry conditions, from 350 to 550 °C—first dry cycle; (2) a run under wet conditions (2 vol.% $H_2O$), from 400 to 550 °C—2% water; (3) a run in dry conditions after the suppression of water from gas stream, from 350 °C to 550 °C—second dry cycle.

Formation of nitrogen was used to calculate NO conversion and methane conversion was obtained by following the change in the methane peak area.

## 3. Results

### 3.1. XRD analysis

X-ray diffraction analysis performed for all studied samples shows that they preserve their crystallinity after metal loading and steaming pre-treatments. Fig. 1 exhibits the X-ray patterns for H-BEA, PdCo-HBEA and for the steamed catalysts at 500 °C. In these XRD patterns PdO, $Co_3O_4$ and CoO are not detected.

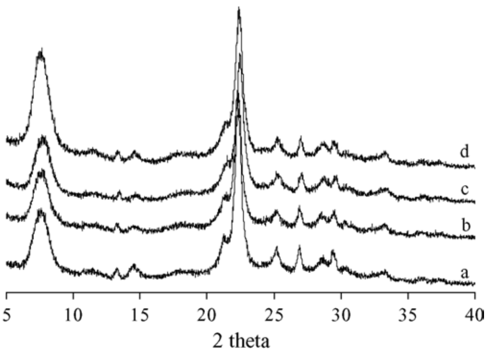

Fig. 1. DRX patterns of fresh samples: (a) H-BEA; (b) PdCo-HBEA; (c) st510; (d) st520.

### 3.2. FTIR analysis

FTIR analysis reveals that no significant dealumination occurs for the non-steamed sample. For the steamed samples the following dealumination is observed: st410, 14%; st510, 19% and st520, 38%. These results evidence the existence of extra framework aluminum in all the catalysts submitted to steaming pre-treatments.

### 3.3. NO SCR with $CH_4$

All catalysts presented in this study were tested in the selective catalytic reduction of NO with methane in the presence of oxygen excess under dry and wet conditions.

Fig. 2 shows that the introduction of Pd in the monometallic catalyst, Co-HBEA, results in a decrease of NO conversion under dry conditions. PdCo-HBEA catalyst exhibits a very poor activity (NO conversions below 20%) when it is tested in absence of water. When the reaction is performed under wet conditions (2% $H_2O$), the conversion decreases at lower temperatures but at 550 °C it preserves the conversion obtained under dry conditions. Moreover, an unexpected increase of NO conversion was observed in the second dry cycle.

These first results obtained after contacting PdCo-HBEA catalyst with water vapor led us to consider a possible improvement in its catalytic behavior by performing different hydrothermal pre-treatments (steaming) on the fresh PdCo-HBEA sample. Those pre-treatments occurred at 400 °C and 500 °C, with 10% of water vapor and at 500 °C with 20% of water vapor (see Table 1). Fig. 3A exhibits catalysts behavior under dry conditions (first dry cycle) and Fig. 3B under wet conditions. Steamed catalyst st410 reveals a moderate improvement in NO conversion into $N_2$ at

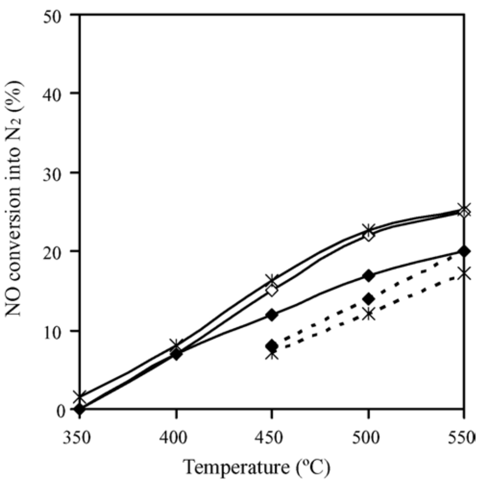

Fig. 2. Conversion of NO into $N_2$: first cycle under dry conditions for Co-HBEA (–*–) and PdCo-HBEA (–◆–); 2% water Co-HBEA (- -*- -) and PdCo-HBEA (- -◆- -); second cycle under dry conditions for PdCo-HBEA (◇) after the removal of water from gas stream. NO, 1000 ppm; $CH_4$, 2000 ppm; $O_2$, 5%; GHSV = 45,000 $h^{-1}$.

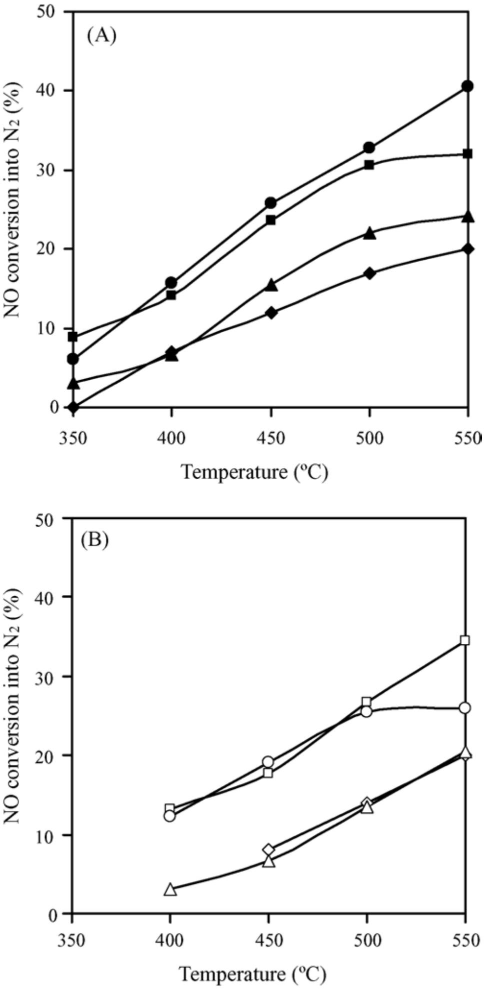

Fig. 3. Conversion of NO into $N_2$ for: PdCo-HBEA (◆); st410 (▲); st510 (■); st520 (●). (A) Dry conditions and (B) wet conditions.

temperatures above 450 °C and in absence of water. Under wet conditions, the behavior was quite similar to the one obtained with PdCo-HBEA catalyst. On the contrary, catalysts steamed under more severe conditions (500 °C) – st510 and st520 – reveal, when tested under dry conditions, a significant increase in NO conversion when compared with PdCo-HBEA, even at low reaction temperatures. Under wet conditions, these steamed catalysts did not exhibit a significant loss of activity.

Fig. 4 shows the results of NO conversion into $N_2$ observed at 550 °C for the studied catalysts in each one of the reaction cycles. All catalysts evidence an increase in conversion after being exposed to the reactant mixture with 2% of water vapor except for catalyst st520. This catalyst presents a significant catalytic improvement compared with the PdCo-HBEA but its stability was greatly affected by presence of water and the initial conversion (first dry cycle) was not restored after the removal of water from gas stream (second dry cycle). On the contrary catalyst st510 shows not only a significant improvement in the catalytic activity (under dry and wet conditions), but also an increase in stability.

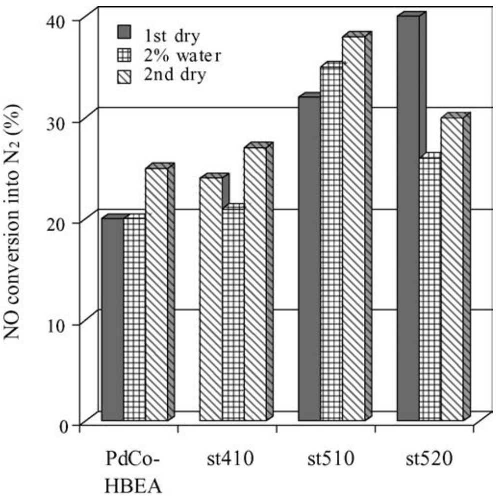

Fig. 4. NO conversion into $N_2$ for all catalysts at 550 °C for a complete run of cycles of approximately 30 h on gas stream.

For total methane oxidation, the catalytic performance is quite similar for all the studied catalysts. Fig. 5 compares the catalytic behavior at 550 °C for a complete run of cycles with all catalysts. Methane conversion observed for all catalysts is in the range 30–40%, meaning that it is not greatly affected by the changes induced by steaming or by the presence of water vapor in the reaction mixture.

Selectivity towards $N_2$ is defined as a fraction of the reducing agent used to reduce NO into $N_2$, i.e., the ratio of the consumption rate of methane for NO reduction to the total consumption rate of methane [6]. Fig. 6 shows that hydrothermal treatments play an important role in what catalysts selectivity is concerned. The enhancement of selectivity is observed in dry (Fig. 6A) and wet (Fig. 6B) conditions, mainly for the catalysts submitted to more severe pre-treatments. Under wet conditions this improvement is more significant.

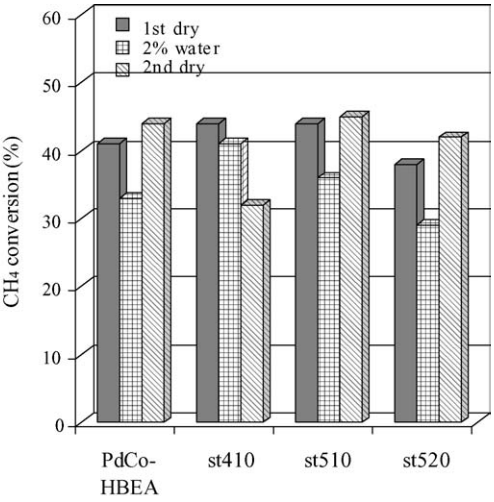

Fig. 5. Total $CH_4$ conversion for all catalysts at 550 °C for a complete run of cycles of approximately 30 h on gas stream.

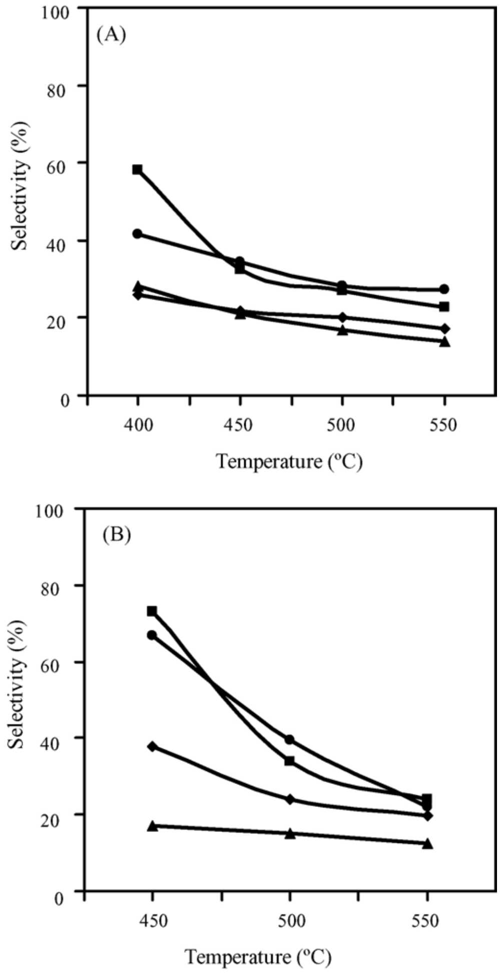

Fig. 6. Selectivity towards $N_2$: PdCo-HBEA (◆); st410 (▲); st510 (■); st520 (●). (A) Dry conditions and (B) wet conditions.

### 3.4. UV–vis analysis

Fresh and used catalysts were analyzed by UV–vis in order to evaluate the effect of steaming pre-treatments in the relative distribution of $Co^{2+}$ in the three exchange sites α, β and γ as proposed by Dědeček et al. [24] in BEA structure. Nevertheless, in a recent paper [27], this assignment was considered doubtful because authors found similar spectra for Co-silica-alumina and Co-H-zeolites. Fig. 7 shows the visible spectra of all fresh samples. The deconvolution of the spectra of PdCo-HBEA into the Gaussian bands of the spectral components α, β and γ was performed according to the literature [24] and is illustrated in Fig. 8. The ratio of the integral intensities of the individual bands of the spectral components (β and γ) was found to be similar for all the studied samples: ~0.3 to ~0.6 to 1 to 0.2 for β and ~0.6 to 1 for γ. Results are presented in Table 2, which reveals that β exchange sites are the most occupied in any case (even in the spent catalysts—not shown). Only slight differences in the relative occupation by cobalt ions are detected related to both Pd introduction and steaming treatments.

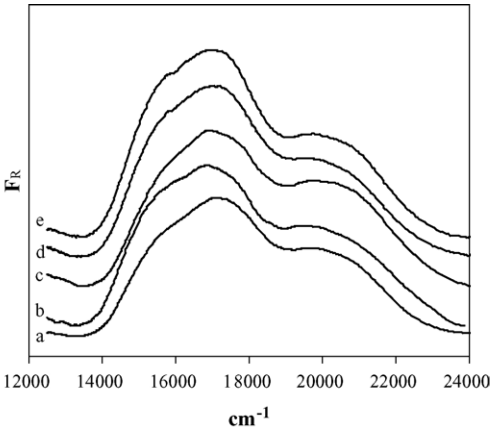

Fig. 7. Normalized visible spectra of fresh samples: (a) Co-HBEA; (b) PdCo-HBEA; (c) st410; (d) st510; (e) st520.

### 3.5. $H_2$-TPR analysis

$H_2$-TPR profiles for fresh samples, Co-HBEA and PdCo-HBEA are exhibited in Fig. 9A. With the purpose of identifying the temperature of $Co_3O_4$ reduction process, a

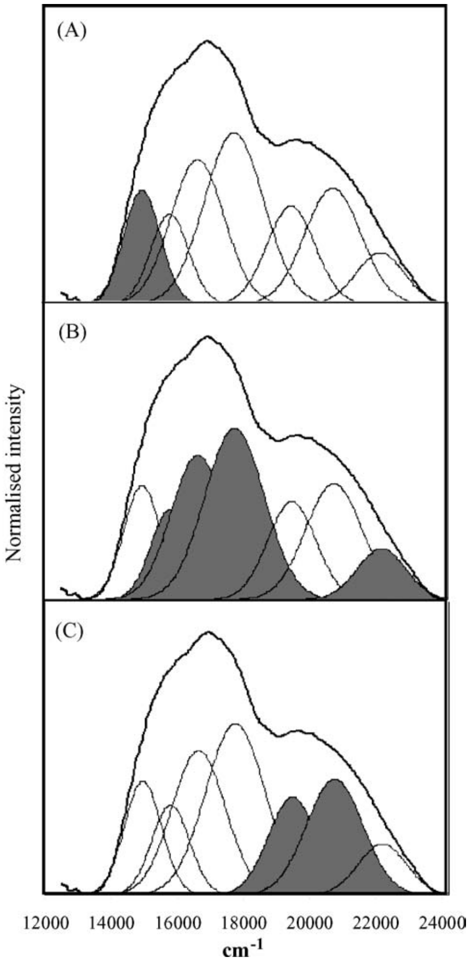

Fig. 8. Decomposition of the visible spectra of PdCo-HBEA to Gaussian curves, individual components are indicated by a shadow area: (A) component α; (B) component β; and (C) component γ.

Table 2
Relative distribution in α, β and γ sites of $Co^{2+}$ cations

| Catalyst | α | β | γ |
|---|---|---|---|
| Co-HBEA | 11 | 63 | 26 |
| PdCo-HBEA | 11 | 60 | 29 |
| st410 | 7 | 62 | 31 |
| st510 | 13 | 63 | 24 |
| st520 | 7 | 67 | 26 |

mechanical mixture with HBEA was also prepared and presented in this figure. In Fig. 9B TPR profiles for the fresh steamed samples are shown.

Co-HBEA sample only presents a high-temperature reduction process, with a maximum at about 990 °C, attributed to the reduction of $Co^{2+}$ ions located at charge compensation sites [28]. For PdCo-HBEA catalyst this reduction process shifts for lower temperatures (maxima at 720 °C) what has been related to the presence of metallic palladium ($Pd^{2+}$ is reduced to $Pd^0$ at low temperatures—peak at 80 °C), capable to activate $H_2$ and promote the reduction of cobalt species [29].

TPR profile corresponding to the mechanical mixture with pure $Co_3O_4$ shows that the reduction of this oxide corresponds to a process with a peak maximum at about 350 °C.

PdCo-HBEA as well as steamed catalysts present several reduction processes between 100 °C and 500 °C that have been assigned to different types of cobalt oxides: (i) between 150 °C and 300 °C reduction processes are assigned to cobalt oxide species that interact with zeolite protons, Co-oxo ions [7,28]; (ii) $Co_3O_4$ in different Co and PdCo-zeolite structures has been identified with a reduction process around 385 °C [8,28–30] which is consistent with the result we obtained for the mechanical mixture $Co_3O_4$/HBEA; (iii) peaks between 425 °C [28] and 600 °C [8] had been ascribed, as for other structures, to cobalt oxide species inside the pores of the zeolite, more difficult to reduce [31].

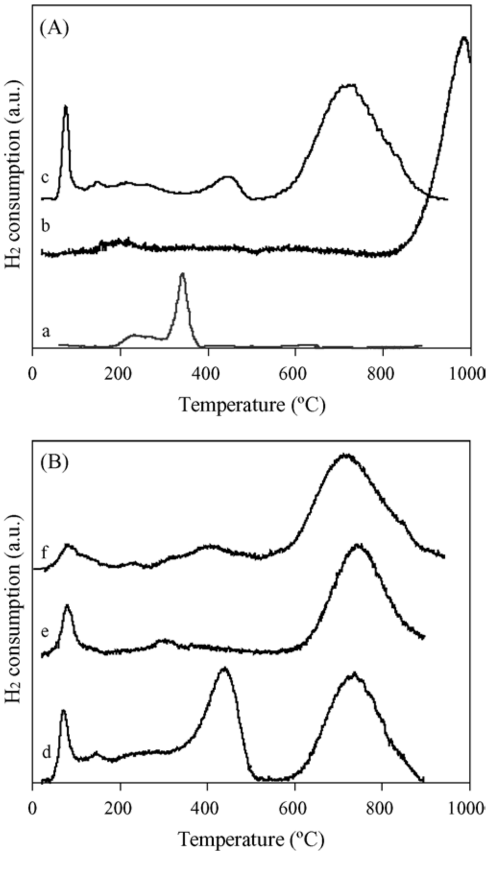

Fig. 9. $H_2$-TPR profiles of (A) non-steamed catalysts: (a) $Co_3O_4$/H-BEA; (b) Co-HBEA; (c) PdCo-HBEA; and (B) steamed catalysts: (d) st410; (e) st510; (f) st520.

The reduction processes observed with PdCo-HBEA and st410, around 450 °C, is then suggested to be related with the reduction of cobalt oxides located inside the zeolite structure. On the other hand, no reduction peak at 350 °C is detected. This means that, probably, no significant amount of $Co_3O_4$ is present in bimetallic samples.

Reduction of palladium species is observed at temperatures around 80 °C, corresponding to a sharp peak. This process is generally slightly shifted to higher temperatures with the severity of steaming and, simultaneously, a change in intensity and peak width can be detected.

An attempt to quantify $H_2$ consumption was made. Peak positions (maxima temperatures) and the H/Metal atomic ratios are presented in Table 3. Assuming that the peak at higher temperatures (720 °C) corresponds to the complete reduction of $Co^{2+}$ ions to $Co^0$, the H/Co ratio would be equal to 2. On the other hand, the complete reduction process of $Co_3O_4$ species lead to an H/Co ratio of 8/3; this value is reached for the mechanical mixture (Fig. 9A(a)). Therefore, the measured value for hydrogen consumption involved in the reduction processes of Co species is quite low. The gap between the expected and the obtained ratio can be attributed to the presence of Co species that cannot be reduced below 900 °C. This fact has already been reported by several authors [8,24,28].

For the reduction of palladium species an H/Pd = 2 was expected. Table 3 shows that all fresh catalysts reached this value, except for st520.

In general, the quantification of hydrogen consumption in fresh samples reveals: (i) a low value of H/Co ratio, suggesting that a considerable fraction of cobalt species is not detected; (ii) an almost constant value for H/Pd ratio equal to 2 corresponding to the complete reduction of Pd.

All spent catalysts were also characterized by $H_2$-TPR. In Fig. 10 these profiles are presented and compared with fresh samples.

Non-steamed PdCo-HBEA catalyst shows (Fig. 10A), after reaction, the disappearance of the cobalt oxide species that are reduced at about 450 °C. Simultaneously, an increase of species reducible at lower temperatures is observed. The fraction of $Co^{2+}$ (in exchange sites) reduced in both samples (see Table 3) is similar. An increase of the intensity of the reduction process in the low-temperature range (formally assigned to palladium species) is also observed.

Spent catalyst st410 exhibits (Fig. 10B) a significant decrease of the cobalt oxide species reducible at about

Table 3

$H_2$-TPR results for the studied catalysts

| Catalyst | Peak 1 (°C) | Peak 2 (°C) | Peak 3 (°C) | Peak 4 (°C) | H/Co total | H/"Pd" |
|---|---|---|---|---|---|---|
| $Co_3O_4$ | 345 | – | – | – | 2.7 | – |
| Co-HBEA[a] | – | – | – | 990 | – | – |
| PdCo-HBEA | 80 | 150–300 | 450 | 720 | 1.1 | 2.0 |
| PdCo-HBEA[b] | 80 | 150–300 | – | 750 | 1.4 | 3.2 |
| st410 | 75 | 150–300 | 450 | 740 | 1.6 | 2.0 |
| st410[b] | 111 | 150–300 | 450 | 740 | 1.4 | 3.8 |
| st510 | 80 | 150–300 | – | 740 | 0.8 | 2.0 |
| st510[b] | 130 | 150–300 | – | 775 | 1.2 | 5.4 |
| st520 | 90 | 235 | 411 | 730 | 0.9 | 1.7 |
| st520[b] | 70–125 | 150–300 | – | 780 | 1.1 | 7.8 |

[a] Not quantified due to incomplete reduction process.

[b] Spent catalysts.

450 °C. A very important change is also detected in the region usually assigned to Pd reduction: a shift of the peak maxima to higher temperature and a remarkable increase of its intensity and width. No significant changes are detected in the fraction of reduced $Co^{2+}$.

With catalyst st510 (Fig. 10C) the more evident modification also concerns the region assigned to Pd reduction: a shift of the peak maxima to higher temperature and a notorious increase of its intensity and width. Some redistribution of cobalt oxides is also detected, namely an enhancement of the species located in the low-temperature region (150–300 °C). No significant changes are detected in the fraction of reduced $Co^{2+}$. With st520 catalyst these effects are also present (Fig. 10D).

In general, the quantification of hydrogen consumption in spent samples reveals: (i) a low value of H/Co ratio, indicating that (as already observed in fresh samples) a considerable fraction of cobalt species is not detected; (ii) the attainment of unexpected high values for H/Pd ratio specially in the samples obtained under more severe steaming conditions.

## 4. Discussion

The improved catalytic results first obtained with the non-steamed PdCo-HBEA catalyst are a direct consequence of its exposure to the reaction mixture, containing 2% of water vapor. Subsequent hydro-treatments performed under more severe conditions (steaming), confirm the positive effect of the contact of the bimetallic catalyst with water vapor, at high temperature. This enhancement suggests alterations suffered both by metal species and/or by zeolite structure.

### *4.1. Palladium species on PdCo-HBEA catalysts*

Although there is no consensus in the literature about the exact nature of the active Pd sites for $CH_4$-SCR [29],

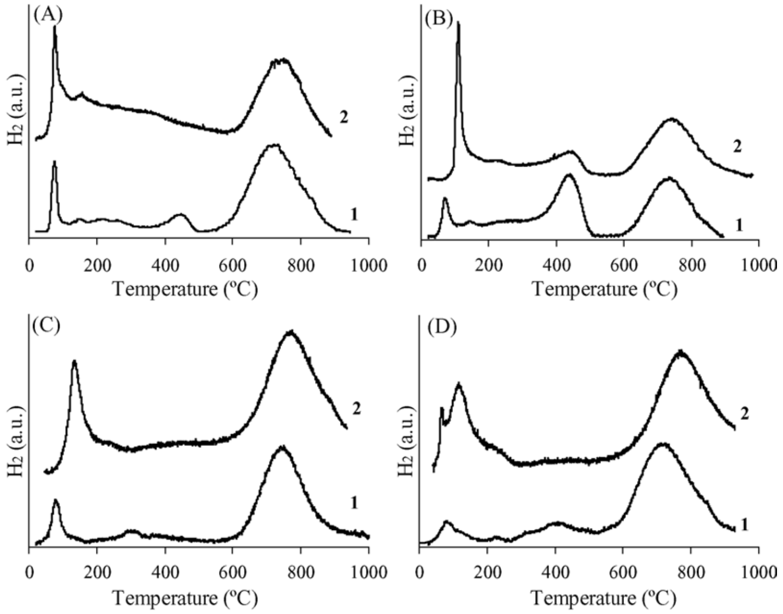

Fig. 10. $H_2$-TPR profiles of (A) PdCo-HBEA; (B) st410; (C) st510; (D) st520: (1) fresh samples; (2) spent samples.

different authors [32] suggest that hydroxide adducts of palladium $[Pd(OH)^+]$ can compensate the negative charges associated to zeolite exchange sites. The formation of isolated oxo and/or hydroxo Pd(II) complexes and, under steady-state conditions, the co-existence of clusters of metallic palladium has also been observed [33]. On the other hand, the location of $Pd^{2+}$ ions on zeolite structure is still subject of discussion, authors suggesting that it should be different from the one observed for cobalt bare ions [29].

In $CH_4$-SCR, the presence of palladium in bimetallic Pd-Co-zeolite catalysts is known to improve both the activity and selectivity, and synergetic effects between cobalt and palladium (incorporated in conditions similar to those chosen in this work, i.e., via ion-exchange) were proposed to explain the enhancement performance compared with single-metal systems [8,34,35].

However, catalysts studied in this work present a different behavior: (1) the incorporation of palladium in Co-HBEA catalyst lead to a decrease in NO SCR activity and no promotion in the selectivity towards $N_2$ is detected when non-steamed catalyst is tested in dry conditions; (2) only after the most severe steaming pre-treatments, increased values of activity, selectivity and stability (namely under wet conditions) are attained. In view of the present results, we can assume that Pd-Co synergetic effect (that has been considered as responsible by the enhancement of the activation of methane that can occur at lower temperature, in comparison to Co-zeolites or to an increase of NO oxidation [8,35]), is only observed for PdCo-HBEA steamed under more severe conditions.

Another aspect that cannot be overruled, concerns the possible formation of PdO under steaming conditions. Some authors [36] showed that the presence of water vapor in contact with Pd-MOR and Pd-ZSM/5 catalysts results in deactivation caused by agglomeration of palladium to form PdO, that is reported to reduce around 200–250 °C [29,34–36]. PdO is known for the high methane combustion activity [37]. It is clear that no significant amount of PdO is formed in steamed samples, which is in good agreement with the observed increase in selectivity.

### 4.2. Cobalt species on PdCo-HBEA catalysts

The calculated high values of H/Metal ratio in the temperature range of palladium reduction (80–150 °C) strongly suggest the appearance of cobalt species with reduction temperatures very similar to those observed for palladium. This can arise from: (1) the formation of cobalt oxide species; (2) the migration of non-reducible cations and/or oxides towards more reducible locations [8]. It should be remembered that a significant part of cobalt species is not detected by $H_2$-TPR analysis and also that the species reducible at 450 °C decrease (spent st410) or practically disappear (st510, st520) under more severe steaming conditions. As no major differences are observed in $Co^{2+}$ ions region, it is clear that steaming treatment (and consecutive reactivity tests, where catalysts are brought until 550 °C, under a reaction mixture that contains 2% of water and 5% of oxygen) induces cobalt oxide to migrate and/or to be formed in such a way that they become reducible at lower temperatures. This redistribution process would be induced by the presence of water molecules at high temperature. This possibility was suggested by Wen and Sachtler [4] that claim an important role of water in increasing the mobility of cobalt species inside zeolite structure.

The formation of low-temperature reducible cobalt species seems to constitute the key factor resulting from the catalysts modifications induced by steaming pre-treatments. The assignment of these species to a particular type of oxide is not obvious. Literature indicates that Co-oxo ions are, among the detected cobalt oxide species, those presenting the lowest reducing temperature (around 230 °C, below the observed for $Co_3O_4$) [7,28,30]. These species are reported in the literature as possibly involved in $CH_4$-SCR of NO reduction mechanism (NO oxidation at low temperatures) [28,31]. It is possible to suggest that Co-oxo ions can be involved on the detected overlapping with palladium reduction process; nevertheless, taking in account the very low reduction temperature of these species, it is assumed that they can correspond to cobalt oxides much easier to reduce, like very small oxide crystals or located in the vicinity of palladium. These small sized oxide particles have been detected, by TEM, in other zeolite structures with similar Co and Pd loading [38].

A slight increase of the temperature of Pd species reduction is also observed, suggesting some sort of direct interaction between them and Co-oxo ions; the formation of multi-metallic entities, already suggested [39] should be considered. In this case, the role of extra-framework aluminum cannot be ruled out.

High-temperature reduction peaks, assigned to $Co^{2+}$ ions are quite similar for all fresh and spent catalysts. However, a shift upward by about 30 °C in the sequence: PdCo-HBEA $\sim$ st520 $<$ st410 $<$ st510 is observed in fresh catalysts. This fact was already reported [4] on steamed Co-MFI catalysts and a direct relation was made by the authors with the observed increase in catalytic performance. The results obtained in our work are quite similar; however, no significant change in the relative distribution of $Co^{2+}$ detectable by UV–vis analysis was found. In any case, it must be mentioned that in steamed PdCo-HBEA catalysts, the displacement of the maxima of the reduction peak of $Co^{2+}$ does not constitute the only modification observed and capable of explaining the increase of their performance.

### 4.3. Modifications in zeolite structure

As far as zeolite structure modifications are concerned, no detectable dealumination (i.e., migration of lattice aluminum towards extra-framework positions) was observed for the non-steamed sample, even after catalytic tests. On the contrary, as expected, increasing dealumination was detected for samples submitted to severe steaming at 500 °C with 10% and 20% water vapor. In general, this structural dealumination occurs rather easily and a standard calcination is able to convert significant amounts of Al from tetrahedral to octahedral coordination [40] with deposition of extra-framework Al species (EFAL) on the zeolites channel walls, with a consequent modification in the number of available Brönsted and Lewis acid sites [19,22,40,41].

The effect of Lewis acid sites or EFAL species, in this type of SCR reactions has not been enough explored, but under these thermal treatments conditions, it is possible to envisage a reaction between EFAL species and Co species, leading to the formation of cobalt aluminate compounds (mixed oxides, spinels). $Co_2Al$-oxide is reported to reduce around 470 °C [42] what is quite close to the reduction temperature (450 °C) of the species detected in fresh PdCo-HBEA and in both fresh and spent st410 catalyst (Fig. 10A and B); anyway, this process is not observed in the more dealuminated samples (Fig. 10C and D). Besides this hypothesis, we cannot exclude the effect of steam on reorganization of framework Al, even when the steam conditions are not very strong, as it happens during SCR reaction performed with 2% of water. Recently, Căpek et al. [13] showed that the distribution of Al atoms in Beta zeolite framework controls the state and distribution of Co ion species, which determine their activity in SCR-NO. Single Al atoms in the framework of BEA zeolite are demanded for formation of Co ions highly active under the presence of water vapor.

### 4.4. Particular features of $CH_4$-SCR over PdCo-HBEA catalysts

A common characteristic in HC-SCR is that $NO_x$ conversion always reaches a temperature of maximum activity, which is usually related to a decrease in the availability of the reducing agent due to the non-selective HC total combustion with oxygen at high temperatures.

In the system studied in the present work there is no a well defined maximum in the activity curve, within the temperature range studied here, which is in good accordance with the fact that the conversion of $CH_4$ is, in any case, always inferior to 45%, without a lack of reducing agent. It means that in contrast with what is observed in other PdCo-zeolite catalysts, the temperature range used in this work (350–550 °C) is not enough to promote the complete conversion of methane. This suggests that in this particular zeolite structure, the active species have poor activity and/or that at least one of the stages of the complex reaction pathways (NO selective reduction and $CH_4$ total combustion) acts as a strong rate-limiting step: oxygen or methane activation can be suggested, as they are involved in both pathways.

### 4.5. Influence of catalysts modifications on $CH_4$-SCR results

The interpretation of the effect of described modifications on the basis of proposed reaction mechanisms will be attempt in this point.

#### 4.5.1. $CH_4$-SCR of NO mechanisms

In a very simplified way, three main groups of HC-SCR reaction schemes are proposed in the literature: (1) catalytic decomposition of NO over a reduced metal site, the role of HC being to regenerate the active site; (2) formation of partially oxidized hydrocarbon intermediates (by reaction with oxygen or $NO_2$) that further react with $NO_x$ to yield $N_2$; and (3) oxidation of NO to $NO_2$, followed by the reduction of $NO_2$ to $N_2$ by hydrocarbons, possibly via an organic-nitrogen containing (-nitro, -nitrous) intermediate [15–18].

Recently, the concept of three-function catalysts was proposed to describe the reaction pathway of $deNO_x$ reactions in lean conditions and in the presence of hydrocarbons as reducing agents, thus linking the catalytic functions with specified active sites [15,43]. For $CH_4$-SCR over PdCo-ZSM-5 and PdCo-HMOR, authors suggest that $NO_2$ formation is the first key step that occurs over $Co_3O_4$, the partial oxidation of methane by $NO_2$ occurs over palladium species (PdO) and the reduction of NO by the partially oxidized organic species over $Co^{2+}$ ions in bare positions.

However, other authors [39] claim that, over PtCo-MFI catalyst, $Co_3O_4$ is an undesired species because it only promotes methane oxidation with oxygen instead of $NO_2$. These authors suggest that NO oxidation to $NO_2$ occurs over Pt-Co clusters (the later in the form of highly dispersed $Co_xO_y$), methane being activated in neighbor Co cations. Sachtler and co-workers [28] propose that Co-oxo ions are even more efficient than cobalt oxide particles in converting NO into $NO_2$. Other authors refer [8] that catalysts impregnation with Pd leads to the existence of both $Pd^{2+}$ cations next to PdO agglomerates that are known for a high methane combustion activity [37]. On the contrary, the zeolite stabilized $Pd^{2+}$ ions activate methane and catalyze the $CH_4$-SCR of $NO_x$ [17]. In a recent paper [44] authors showed that $Pd^0$ clusters, that can be present even under strong oxidation conditions can chemisorb methane with dissociation, thus favoring the methane activation.

#### 4.5.2. $CH_4$-SCR catalysis over steamed PdCo-HBEA zeolites

From the results of the present work, it is clear that increasing hydro-treatments severity originates an increase of low-temperature reduction cobalt species. These species were previously assigned to Co-oxo ions, highly dispersed cobalt oxides eventually interacting directly with palladium or corresponding to the formation of multi metallic Pd-Co entities (eventually favored by the presence of extra-framework aluminum). All these species are claimed to be active in the oxidation of NO into $NO_2$. Their presence can explain the enhancement of NO conversion, especially at lower temperatures, observed in steamed samples. The fact that bare $Co^{2+}$ ions, assigned to the reduction of $NO_x$, remain almost untouched with steaming treatments, suggest a possible change in the rate-limiting step in the SCR reaction mechanism, as consequence of the increasing amount of low-temperature reduction cobalt species. Furthermore, these oxide species seem to be stabilized by steaming and reaction in wet conditions, explaining the increase of stability observed in catalysts performance.

As $CH_4$ conversion remains similar in all studied temperature range, regardless of the steaming pre-treatments, it is also possible to infer a moderation effect on methane direct oxidation, promoted by steaming and resulting from an eventual Pd-Co interaction. This could explain the increase of selectivity towards $N_2$ observed for steamed samples.

Nevertheless, it is clear that additional information about the process involved in the formation of these low-temperature reducible species seems to be necessary to give insight about the formation of SCR active species in this particular system.

## 5. Conclusions

PdCo-HBEA zeolite-based catalysts present only poor activity and selectivity for $CH_4$-SCR of NO in the presence of oxygen excess. However, an increase of stability has been detected after testing under wet conditions. Steaming samples revealed an enhancement of activity, selectivity and stability. This behavior is more evident after more severe steaming conditions.

The observed enhancement in the performance of steamed catalysts could be due to: (i) a redistribution of cobalt species with the formation and stabilization of low-temperature reducible oxo-ions what is consistent with an increase of the oxidation of NO into $NO_2$, explaining the global increase of activity, especially at low reaction temperatures; (ii) the maintenance of the reducible amount of $Co^{2+}$ ions in bare positions; (iii) an eventual direct interaction of cobalt and palladium species, that can give rise to a slight restrained activity of total $CH_4$ oxidation by palladium species, partially explaining the increase of selectivity in steamed samples. The fact that $Co^{2+}$ ions remain almost untouched with steaming treatment, suggests a change in the rate-limiting step in the reaction mechanism what is also supported by the increase of more accessible Co oxide species.

A suitable balance between the different active sites seems to constitute a key factor regarding a future improvement in catalysts performance.

## References

[1] W. Held, A. Konig, T. Richter, L. Poppe, Soc. Autom. Eng. Paper 900496, 1990.
[2] M. Iwamoto, H. Hamada, Catal. Today 10 (1991) 57.
[3] Y. Li, J.N. Armor, Appl. Catal. B 1 (1992) L31.
[4] B. Wen, W.M.H. Sachtler, Catal. Lett. 86 (2003) 39.
[5] C. Torre-Abreu, C. Henriques, F.R. Ribeiro, G. Delahay, M.F. Ribeiro, Catal. Today 54 (1999) 407.
[6] Y. Li, J.N. Armor, Appl. Catal. B 3 (1993) L1.
[7] F. Bustamante, F. Córdoba, M. Yates, C. Montes de Correa, Appl. Catal. A 234 (2002) 127.
[8] J.A.Z. Pieterse, R.W. van den Brink, S. Booneveld, F.A. de Bruijn, Appl. Catal. B 39 (2002) 167.
[9] K. Kagawa, Y. Ichikawa, S. Iwamoto, T. Inui, Catal. Lett. 52 (1998) 145.
[10] T.J. Lee, I.-S. Nam, S.W. Ham, Y.S. Baek, K.H. Shin, Appl. Catal. B 41 (2003) 115.
[11] M. Ogura, S. Kage, T. Shimojo, J. Oba, M. Hayashi, M. Matsukata, E. Kikuchi, J. Catal. 211 (2002) 75.
[12] P. Ciambelli, P. Corbo, M. Gambino, F. Migliardini, G. Minelli, G. Moretti, P. Porta, Stud. Surf. Sci. Catal. 97 (1995) 295.
[13] L. Căpek, J. Dĕdeček, B. Wichterlová, J. Catal. 227 (2004) 352.
[14] H. Ohtsuka, T. Tabata, O. Okada, L.M.F. Sabatino, G. Bellussi, Catal. Lett. 44 (1997) 265.
[15] G. Djéga-Mariadassou, M. Boudard, J. Catal. 216 (2003) 89.
[16] B. Adelman, T. Beutel, G.D. Lei, W.M.H. Sachtler, Appl. Catal. B 6 (1995) L201.
[17] M. Misono, Cattech 2 (1998) 183.
[18] E.A. Lombardo, G.A. Sill, J.L. d'Itri, W.K. Hall, J. Catal. 173 (1998) 440.
[19] M. Müller, G. Harvey, R. Prins, Micropor. Mesopor. Mater. 34 (2000) 135.
[20] W.E.J. van Kooten, J. Kapteijn, C.M. van den Bleek, H.P.A. Calis, Catal. Lett. 63 (1999) 227.
[21] A.E.W. Beers, J.A. van Bokhoven, K.M. de Lathouder, F. Kapteijn, J.A. Moulijn, J. Catal. 218 (2003) 239.
[22] J.P. Marques, I. Gener, P. Ayrault, J.C. Bordado, J.M. Lopes, F. Ramôa Ribeiro, M. Guisnet, Micropor. Mesopor. Mater. 60 (2003) 251.
[23] Z. Sobalík, J. Dĕdeček, I. Ikonnikov, B. Wichterlová, Micropor. Mesopor. Mater. 21 (1998) 525.
[24] J. Dĕdeček, L. Căpek, D. Kaucký, Z. Sobalík, B. Wichterlová, J. Catal. 211 (2002) 198.
[25] J.R. Sohn, S.J. DeCanio, J.H. Lunsford, D.J. O'Donnell, Zeolites 6 (1986) 225.
[26] C. Coutanceau, J.M. da Silva, M.F. Alvarez, F.R. Ribeiro, M. Guisnet, J. Chim. Phys. 94 (1997) 765.
[27] T. Montanari, M. Bevilacqua, C. Resini, G. Busca, J. Phys. Chem. B 108 (2004) 2120.
[28] X. Wang, H. Chen, W.M.H. Sachtler, Appl. Catal. B 26 (2000) L227.
[29] J.A.Z. Pieterse, R.W. van den Brink, S. Booneveld, F.A. de Bruijn, Appl. Catal. B 46 (2003) 239.
[30] X. Wang, H. Chen, W.M.H. Sachtler, Appl. Catal. B 29 (2001) 47.
[31] L.B. Gutierrez, A.V. Boix, E.A. Lombardo, J.L.G. Fierro, J. Catal. 199 (2001) 60.
[32] L.J. Lobree, A.W. Aylor, J.A. Reimer, A.T. Bell, J. Catal. 181 (1999) 189.
[33] B. Wen, Q. Sun, W.M.H. Sachtler, J. Catal. 204 (2001) 314.
[34] M. Ogura, S. Kage, M. Hayashi, M. Matsukata, E. Kikuchi, Appl. Catal. B 27 (2000) L213.
[35] M. Ogura, Y. Sugiura, M. Hayashi, E. Kikuchi, Catal. Lett. 42 (1996) 185.
[36] H. Ohtsuka, T. Tabata, Appl. Catal. B 21 (1999) 133.
[37] J. Au-Yeung, K. Chen, A.T. Bell, E.J. Iglesia, J. Catal. 188 (1999) 132.
[38] A.P. Ferreira, C. Henriques, M.F. Ribeiro, F.R. Ribeiro, P. Da Costa. G. Djéga-Mariadassou, in preparation.
[39] A. Boix, E.E. Miró, E.A. Lombardo, M.A. Bañares, R. Mariscal, J.L.G. Fierro, J. Catal. 217 (2003) 186.

[40] I. Kiricsi, C. Ffego, G. Pazzuconi, W.O. Parker, R. Millini, C. Perego, G. Bellussi, J. Phys. Chem. 98 (1994) 4627.
[41] J.B. Higgins, R.B. Lapierre, J.L. Schlenker, A.C. Rohrman, J.D. Wood, G.T. Kerr, W.J. Rohrbaugh, Zeolites 8 (1988) 446.
[42] P. Arnoldy, J.A. Moulijn, J. Catal. 93 (1985) 38.
[43] O. Gorce, H. Jurado, C. Thomas, G. Djéga-Mariadassou, A. Khacef, J.M. Cornier, J.M. Pouvesle, G. Blanchard, S. Calvo, Y. Lendresse, SAE Technical Paper 2001 01 3508, 2001.
[44] H.-Y. Chen, Q. Sun, B. Wen, Y.-H. Yeom, E. Weitz, W.M.H. Sachtler, Catal. Today 96 (2004) 1.